Department of Sustainability and Environment

Climate Change in Victoria

Assessment of climate change for Victoria: 2001-2002

Undertaken for the Victorian Department of Sustainability and Environment by the Climate Impact Group, CSIRO Atmospheric Research

Authors: R. Suppiah, P. H. Whetton and I. G. Watterson

April 2004

Important Disclaimer

This report relates to climate change scenarios based on computer modelling. Models involve simplifications of the real physical processes that are not fully understood. Accordingly, no responsibility will be accepted by CSIRO or the Victorian Department of Sustainability and Environment for the accuracy of projections in this report or actions on reliance of this report.

Address for correspondence

Dr Ramasamy Suppiah
CSIRO Atmospheric Research
PMB No 1, Aspendale, Victoria 3195
Telephone (03) 9239 4554
FAX: (03) 9239 4444
E-mail: suppiah.ramasamy@csiro.au

TABLE OF CONTENTS

ACKNOWLEDGMENTS .... **iv**

LIST OF FIGURES .... **v**

LIST OF TABLES .... **vi**

EXECUTIVE SUMMARY **1**

1 Introduction **2**

1.1 Background **2**

1.2 New climate research covered in this report **2**

2 The Assessment of GCM Simulations Over the Southeastern Region of Australia 4

2.1 Average climate simulations **4**

2.2 Patterns of Victorian rainfall variability and associated weather systems: Observations **9**

2.3 Patterns of Victorian rainfall variability and associated weather systems: Current climate models **13**

2.4 Assessment of simulated present-day climate of Victoria by climate models **21**

2.5 Mean sea level pressure changes under enhanced greenhouse conditions **22**

3 Extreme Rainfall Events: A Further Analysis **24**

3.1 Simulations of rainfall change **24**

3.2 Daily extremes of rainfall **25**

3.3 Extreme value relationships inferred from theory **28**

4 Revised Climate Change Scenarios for Victoria **29**

4.1 Average temperature changes **30**

4.2 Regional average rainfall changes **30**

5 Conclusions **32**

6 References **33**

ACKNOWLEDGMENTS

The work of the authors draws upon research findings of many colleagues within CSIRO Atmospheric Research (CAR), and overseas research institutions. CSIRO global climate and regional climate models were developed by the members of the Earth Systems Modelling Program of this Division.

Observational high-quality rainfall and temperature data sets have been provided by Dean Collins and Paul Della-Marta of the National Climate Centre of the Bureau of Meteorology, Melbourne.

Martin Dix provided useful comments on the manuscript. Janice Bathols, Cher Page and Mark Collier of CAR performed data processing, data manipulations and plotting. The layout was designed by Julie Siedses.

Liaison between CAR and the Victorian Department of Sustainability and Environment has been facilitated by Rod Anderson.

This work was produced by CAR under contract to the Victorian Department of Sustainability and Environment. This work also contributes to CSIRO’s Climate Program.

LIST OF FIGURES

Figure 1. Six regions of Victoria considered in this report. 2

Figure 2. Pattern correlation and RMS error for observed versus model temperature (left column) and precipitation (right column) for the models in Table 1. 6

Figure 3. Observed and simulated mean sea level pressure patterns by CSIRO Mark3 and CC50. Observed and simulated climatologies are based on years from 1960 to 2000. The left, middle and right columns show observations from NCEP reanalysis, Mark3 and CC50 simulations respectively, ordered from top to bottom for DJF, MAM, JJA and SON. Units are in hPa. 7

Figure 4. Observed and simulated temperature patterns by CSIRO Mark3 and CC50. Observed and simulated climatologies are based on years from 1960 to 2000.The left, middle and right columns show observations from the Bureau of Meteorology, Mark3 and CC50 simulations respectively, ordered from top to bottom for DJF, MAM, JJA and SON. Units are in °C. 8

Figure 5. Observed and simulated rainfall patterns by CSIRO Mark3 and CC50. Observed and simulated climatologies are based on years from 1960 to 2000. The left, middle and right columns show observation from the Bureau of Meteorology, Mark3 and CC50 simulations respectively, ordered from top to bottom for DJF, MAM, JJA and SON. Units are in mm. 9

Figure 6. Observed relationships between Victoria statewide rainfall and regional rainfall. Correlation coefficients of less than 0.8 (horizontal line) are highlighted as showing independence of regional rainfall variability. 12

Figure 7. Observed relationships between Victoria State-wide rainfall and mean sea level pressure. 14

Figure 8. Observed relationships between northern regions rainfall and mean sea level pressure. 14

Figure 9. Observed relationships between southern regions rainfall and mean sea level pressure. 15

Figure 10. Correlation coefficients between statewide rainfall and regional rainfall for CCCM1, HADCM2 and HADCM3. ANN1, MAM1, JJA1, SON1 and DJF1 indicate values based on model results for annual, autumn, winter, spring and summer, respectively. ANN), MAMO, JJAO,SONO and DJFO show correlations based on observation. 16

Figure 11. Same as in Figure 10, but for ECHAM3, ECHAM4 and GFDL. 17

Figure 12. Same as in Figure 10, but for CCCM2, Mark2 and Mark3. 18

Figure 13. Same as in Figure 10, but for DAR125, DAR60 and CC50. 19

Figure 14. Mean sea level pressure difference between first 40 years and the last 40 years of simulations. Simulations from all available models are used as there is not a single models stands out clearly as best simulating the link between rainfall and circulation patterns. 23

Figure 15. Percentage change in seasonal averages of daily rainfall, from 1961-1990 to 2071-2100 in the CSIRO Mark 2 model (A2): (a) December-February, (b) March-May, (c) June-August, and (d) September-November. 25

Figure 16. Frequency of daily precipitation at the East Victoria grid point, for January days during 1961-1990. Data from five simulations are combined to produce a histogram with bar width 0.1 mm. The dry day frequency, 0.6, is not depicted, as are daily values from 20 mm to the extreme value 40.5 mm. The gamma distribution fitted to the data is shown as a line. 26

Figure 17. Percentage change in seasonal averages of 30-month extremes of daily rainfall (effectively 10-year extremes), from 1961-1990 to 2071-2100 (A2): (a) December-February, (b) March-May, (c) June-August, and (d) September-November. 26

Figure 18. Percentage change in (a) annual mean rainfall and (b) 30-year extremes of daily rainfall, from 1961-1990 to 2071-2100 (A2). 27

Figure 19. Percentage changes in extreme rainfall for the East and West Victoria grid points, plotted against percentages changes in the (a) mean, and (b) the ratio of variance to mean. Values for the four seasons are shown as dots, and the annual values, for the (a) case, are shown as stars. 27

Figure 20. Pattern of annual and seasons warming from an optimal set of nine models (left panels) and from all available twelve models (right panels). Units: Degrees C. Model details are given in Table 1. 29

*Figure 21. Annual and seasonal rainfall changes (in percentage) for Victoria from an optimal set of nine models (left panels) and from all available twelve models (right panels). Model details are given in Table 1.*31

LIST OF TABLES

Table 1: Climate model simulations analysed in this report. Further information about the non-CSIRO simulations may be found at the IPCC Data Distribution Centre (http://ipcc-ddc.cru.uea.ac.uk/). Some further information on the emission scenarios used may be found in Figure 2 of the last year's report (Whetton et al., 2002). 4

Table 2: Correlation coefficients among six regions of Victoria calculated for annual and four seasons using regional rainfall data for 1961-2000. Relatively weak and strong (less than 0.6 and greater than 0.8) correlation coefficients are shown by italics and bold. 11

Table 3. Inter-regional correlation of rainfall variations: model versus observations. A dot indicates a correlation of regional rainfall with state rainfall of less than 0.8 and a cross more than 0.8. Dots thus indicate regions and seasons where region rainfall anomalies show greater independence of statewide anomalies. Seasons are autumn (A), winter (W), spring (S) and summer (S). Northwest and northcentral regions (not shown) show crosses for all cases. 20

Table 4. Global and regional climate models ability to simulate the relationship between large-scale circulation patterns and rainfall over Victoria as a whole and also for subregions of Southeast and Southwest. The capability of the models of simulating the relationship is determined by a threshold value of pattern correlation of 0.4. Dots indicate values greater than 0.4 and crosses less than 0.4. Seasonal results for autumn (A), winter (W), spring (S) and summer (S). 21

EXECUTIVE SUMMARY

This is the second annual climate change report of a three-year consultancy between the Victorian Department of Sustainability and Environment and CSIRO Atmospheric Research aimed at assessing observed and projected climate change in Victoria, its impacts and potential adaptations. In this report, particularly, we have focused on assessing the processes that give rainfall to Victoria and also spatial variability of rainfall simulated by climate models.

Together with previous models' results, we have assessed average climate simulations of new three models to produce revised climate change scenarios. Two of these new simulations are from CSIRO, using the CSIRO Mark3 and Cubic Conformal models.

In this report, we have included revised climate change scenarios for temperature and rainfall changes for Victoria. In the revised scenarios, results from three new simulations are included.

Annual average temperatures over the north and east of the State are projected to be between 0.3 and 1.6^{o}C higher by 2030 and between 0.8 and 5.0^{o}C higher by 2070, relative to 1990. In the south, the ranges are 0.2 - 1.4^{o}C by 2030 and 0.7 - 4.3^{o}C by 2070. The warming is projected to be greatest in summer and least in winter.

Projected annual average rainfall ranges tend toward decrease over most of the state (–15% to +3% in 2030 and –40% to +10% in 2070 in the north, and –9% to +3% in 2030 and–25% to +9% in 2070 in the south). The decreases are strongest in spring through most of the State. On the other hand, over northern Victoria in summer and autumn and over parts of southern Victoria in winter, the direction of rainfall change is uncertain.

The analysis presented in this report has shown that most current models can distinguish different regions of the state in terms of independence in their current rainfall variability. This gives significant additional justification for providing regional detail in simulated rainfall change over Victoria using current models. The potential realism of simulated differences in rainfall change in, say, northern versus southern Victoria, has been enhanced.

Since most of the models simulate decreased rainfall under enhanced greenhouse conditions, we have investigated the link between seasonal rainfall over Victoria and mean sea level pressure over a broad region that encompasses parts of the Indian and Southern oceans and the Australian continent. Simulated spatial correlation patterns were compared with observed patterns. Most of the models simulate observed spatial patterns of correlation during autumn and winter, but only a few models capture the relationship during spring and summer. In this light, the spring and summer projected rainfall changes should be viewed as less reliable, and autumn and winter changes as more reliable.

An analysis of extreme rainfall from CSIRO Mark2 indicates an increase in extreme rainfall under enhanced greenhouse conditions. More significantly, the analysis has indicated that it is likely to be possible to estimate changes in daily extreme rainfall from changes in monthly mean and standard deviation. To be able to do this would enable us to include model to model variations in our projected regional extreme rainfall change – this is a key uncertainty that is not well represented at present

1 Introduction

1.1 Background

This is the second annual climate change report of a three-year consultancy between the Victorian Department of Sustainability and Environment and CSIRO Atmospheric Research aimed at assessing observed and projected climate change in Victoria, its impacts and potential adaptations. The First Annual Report 2001 (Whetton *et al*., 2002) drew upon the latest findings of the Intergovernmental Panel on Climate Change (IPCC), as well as regionally-specific (see figure 1) analysis of a broad range of climate modelling results to provide an assessment of climate change over Victoria. This year's report updates and extends that assessment by incorporating newly available climate model results, improved methods of assessment of model reliability over Victoria, and further analysis of simulated changes in extreme rainfall. These research priorities were recommended in last year's report. This year the consultancy also included CSIRO contributions to impact assessment in the areas of agriculture, biodiversity, water resources, and alpine snow conditions, as well as CSIRO assistance in communication of regional climate change information to various stakeholder groups.

Figure 1. Six regions of Victoria considered in this report.

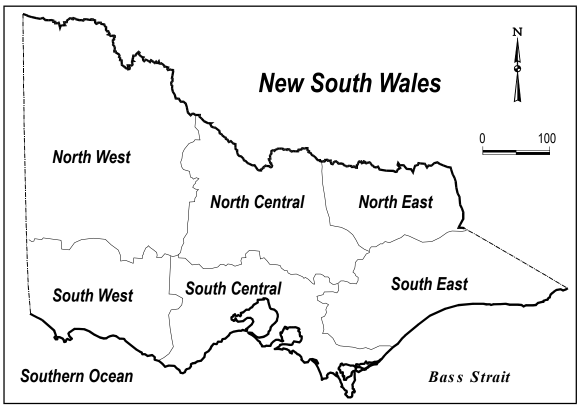

1.2 New climate research covered in this report

Since the release of the first annual report on climate change in Victoria, there were two major developments in modelling capacity at CSIRO Atmospheric Research. The first was the CSIRO Mark3 global climate model (GCM). The horizontal resolution of Mark3 GCM is approximately 200 × 200 km and includes comprehensive cloud micro-physical parameterization, convection parameterization, a dynamic-thermodynamic polar ice model, a land surface scheme with a vegetation canopy, multiple soil types and vegetation types. The Mark3 ocean model is based upon a recent version of the Geophysical Fluid Dynamics Laboratory model. Detailed descriptions of Mark3 GCM can be found in Gordon *et al*. (2002). The Mark3 model represents a major development beyond the previous Mark2 model. Preliminary analyses of model outputs indicate that the model simulates well global-scale patterns of atmospheric circulation, temperature and rainfall. For example, the Mark3 simulation of the El Niño-Southern Oscillation phenomenon is realistic.

The other development is the conformal-cubic global atmosphere model (CCAM). CCAM can be run in stretched-grid mode to provide high resolution over any selected region of interest. Compared to the more traditional nested limited-area modeling approach, it provides great flexibility for dynamic downscaling from any global model, essentially requiring only sea surface temperature and far-field winds from a host model. More detailed information regarding CCAM can be found in McGregor *et al*. (2002).

In this report, first, in addition to various models' performance over the Victorian region provided in last year's report (Whetton *et al*., 2002), information on the assessment of the new generation of CSIRO global and regional models is provided.. Second, the capability of climate models in simulating the spatial variation of current rainfall among the sub-regions of the State (southwest, southeast, etc) is considered. This analysis is aimed at providing an assessment of whether current models have the capability of providing realistic rainfall change information at the sub-regional scale. Third, synoptic circulation patterns that give rainfall to Victorian regions are investigated using observed and simulated data. These analyses are aimed at assessing model performance in simulating rain-producing atmospheric processes. Realistic performance here is also necessary for models to have the capability of reliably simulating enhanced greenhouse changes in rainfall. We also further report on the assessment of extreme rainfall events using multiple simulations of the CSIRO Mark2 GCM. Finally, revised projections of temperature and rainfall changes are given incorporating the newly available model results.

2 The Assessment of GCM Simulations Over the Southeastern Region of Australia

2.1 Average climate simulations

In the last year's report (Whetton *et al*., 2002), we analysed the results of ten models with regard to the simulation of the present climate over the southeastern region of Australia. Here we include data from three further models. This includes the CSIRO Mark3 GCM and CCAM at 50km resolution (CC50), but also results from the Canadian Climate Centre (CCCM2), which had also recently become available. Details regarding the model simulations used in the last year's report and the current report are shown in Table 1**.** Using some summary statistics we show the performance of the simulation of the regional patterns of average temperature and precipitation over southeastern Australia.

Table 1: Climate model simulations analysed in this report. Further information about the non-CSIRO simulations may be found at the IPCC Data Distribution Centre (http://ipcc-ddc.cru.uea.ac.uk/). Some further information on the emission scenarios used may be found in Figure 2 of the last year's report (Whetton *et al*., 2002).

Centre	Model	Emission Scenarios post-1990 (historical forcing prior to 1990)	Years	Horizontal resolution (km)	Symbols used in the report
Canadian CCCM	CCCM1	1% increase in CO_2 p.a.	1900–2100	~400	CCCM1
DKRZ, Germany	ECHAM3/LSG	IS92a	1880-2085	~600	ECHAM3
GFDL	GFDL	1% increase in CO_2 p.a.	1958–2057	~500	GFDL
Hadley Centre, UK	HadCM2	1% increase in CO_2 p.a. (four simulations)	1861–2100	~400	HADCM2
Hadley Centre, UK	HadCM3	IS92a	1861-2099	~400	HADCM3
DKRZ, Germany	ECHAM4/OPYC3	IS92a	1860–2099	~300	ECHAM4
NCAR	NCAR	IS92a	1960-2099	~500	NCAR
CSIRO, Australia	Mark2	IS92a, SRES A2 (four simulations), SRES B2	1881–2100*	~400	MARK2
CSIRO, Australia	DARLAM	IS92a	1961-2100	60	DAR60
CSIRO Australia	DARLAM	IS92a	1961-2100	125	DAR125
CSIRO, Australia	CC	SRES A2	1961-2100	50	CC50
CSIRO, Australia	Mark3	SRES A2	1961-2100	~200	MARK3
Canadian CCCM	CCCM2	SRES	1961-2100	~400	CCCM2

* pre-1990 period common to the SRES simulations

As in previous reports, statistical methods were employed to test whether simulations of these additional new three models for present day greenhouse gas scenarios satisfactorily resemble observed patterns of temperature and precipitation. Simulated and observed patterns for 1961-2000 were compared using a pattern correlation coefficient, which measures pattern similarity, and root mean square error (RMS). As in the previous report, a domain centred on Victoria (135-155ºE, 25-45ºS) was used for testing temperature and precipitation. Seasonal results for temperature and precipitation are shown in Figure 2.

Figure 2 indicates that new simulations of Mark3 and CC50 simulate fairly well the temperature patterns during all seasons. CCCM2 captures observed temperature patterns well during spring and summer, when a continental scale effect on temperature is dominant. However, the pattern correlation for CCCM2 is weak during winter when regional scale influence on temperature is strong over southeastern Australia. CCCM2 also shows weak correlation during autumn compared to other models.

Topographical variations particularly drive the temperature patterns during winter and, not surprisingly, high resolution models perform better. The pattern correlation coefficients between observation and model simulations range from 0.2 to 0.95. Models, which have relatively higher correlations, greater than 0.8, represent the basic regional spatial temperature patterns. However, CSIRO regional climate model simulations (DAR125, DAR60 and CC50), Mark3 and ECHAM4 show strong correlations compared to other models. Figures 3 to 5 depict observed and Mark3 and CC50 simulated mean sea level pressure for the broader Australian region, and temperature and rainfall for a smaller region that encompasses southeastern Australia. It is evident that Mark3 simulates large-scale features of seasonal pressure patterns over Australia, although in some seasons simulated pressure values are a little higher, particularly during JJA. With regard to temperature and rainfall, the higher resolution CC50 does fairly well over the southeast, where topography plays an important role in determining spatial patterns of these parameters. In particular, CC50 simulated rainfall and temperature patterns along the southeast coast show greater realism than the low resolution models shown in this report and also in last year's report.

Figure 2. Pattern correlation and RMS error for observed versus model temperature (left column) and precipitation (right column) for the models in Table 1.

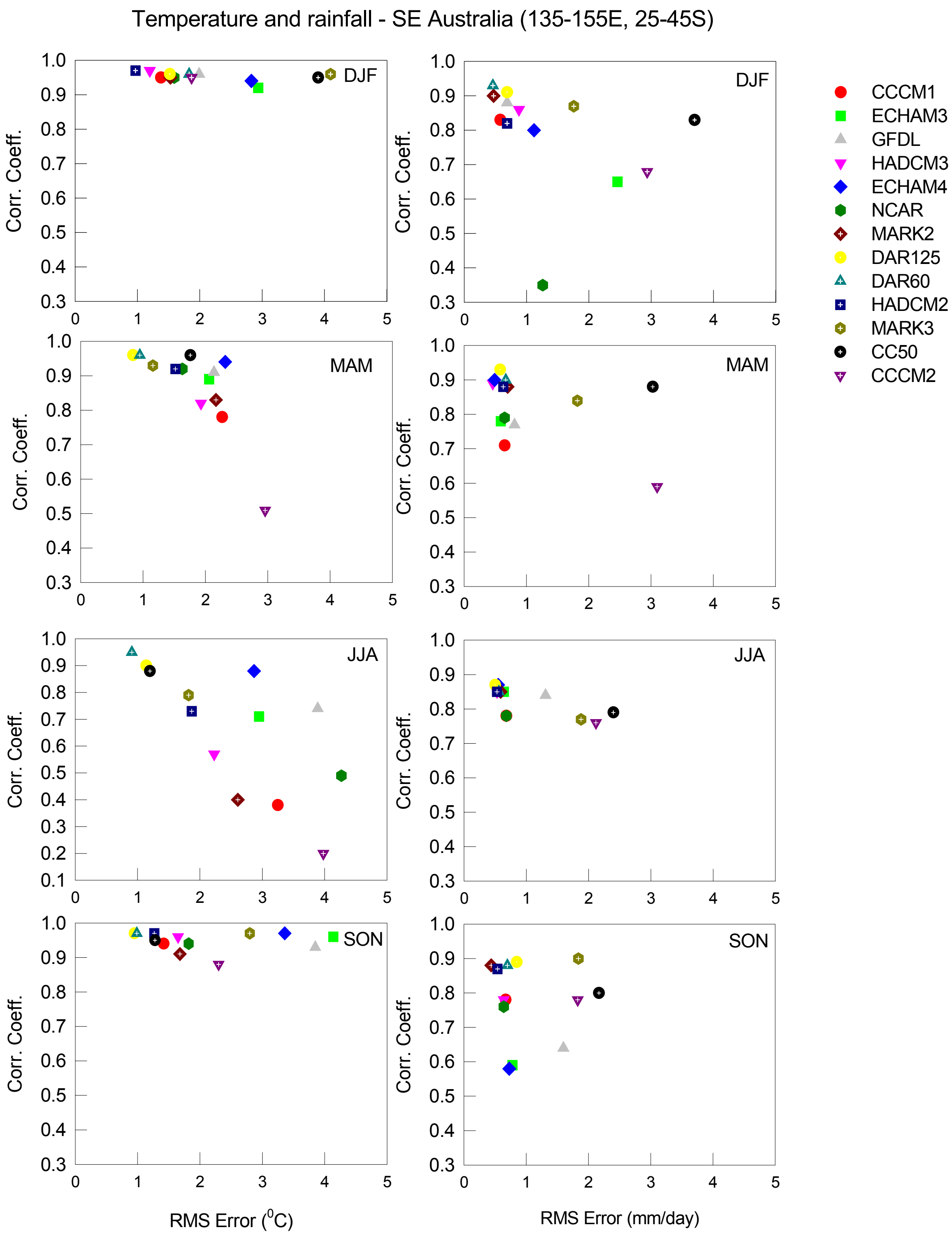

Figure 3. Observed and simulated mean sea level pressure patterns by CSIRO Mark3 and CC50. Observed and simulated climatologies are based on years from 1960 to 2000. The left, middle and right columns show observations from NCEP reanalysis, Mark3 and CC50 simulations respectively, ordered from top to bottom for DJF, MAM, JJA and SON. Units are in hPa.

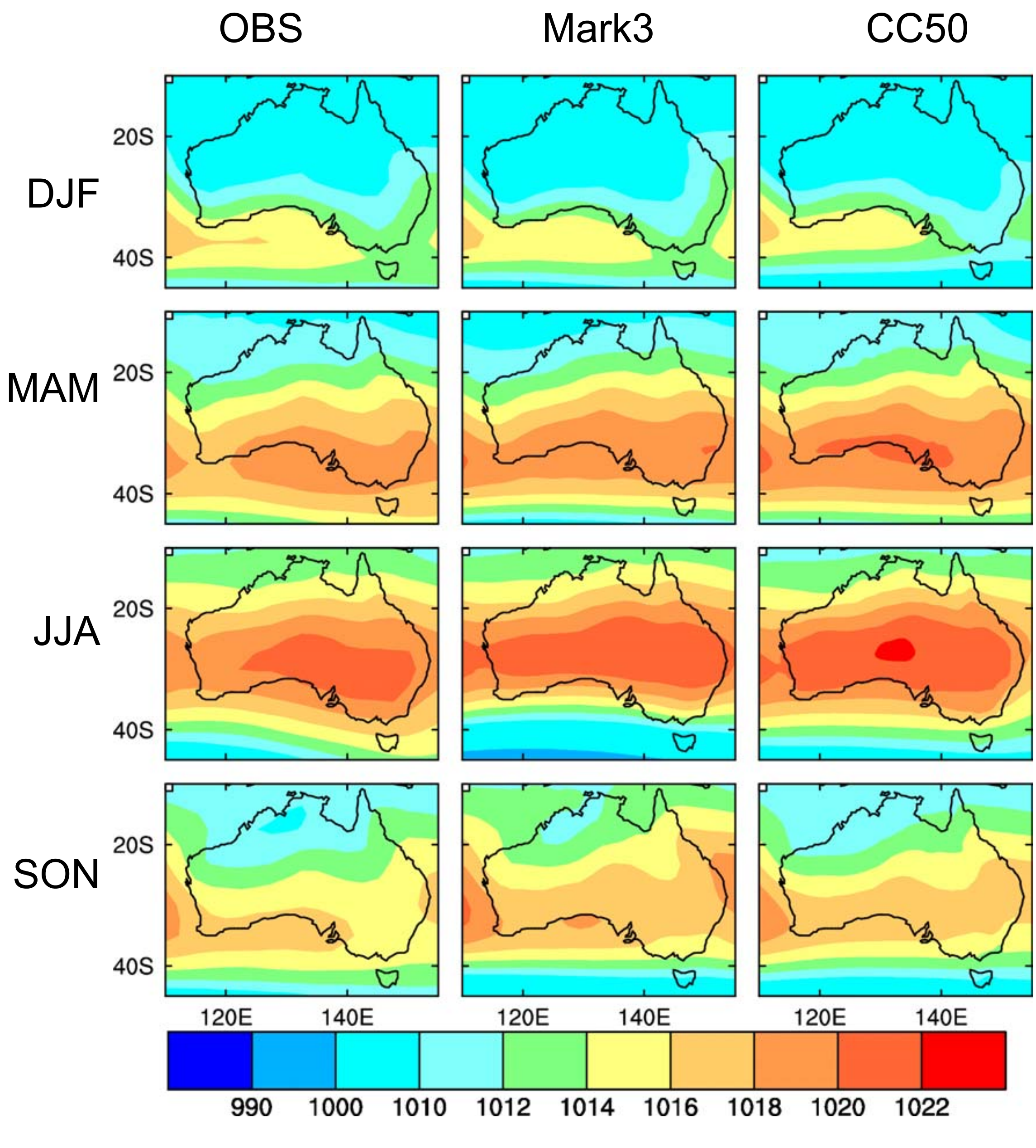

Figure 4. Observed and simulated temperature patterns by CSIRO Mark3 and CC50. Observed and simulated climatologies are based on years from 1960 to 2000.The left, middle and right columns show observations from the Bureau of Meteorology, Mark3 and CC50 simulations respectively, ordered from top to bottom for DJF, MAM, JJA and SON. Units are in °C.

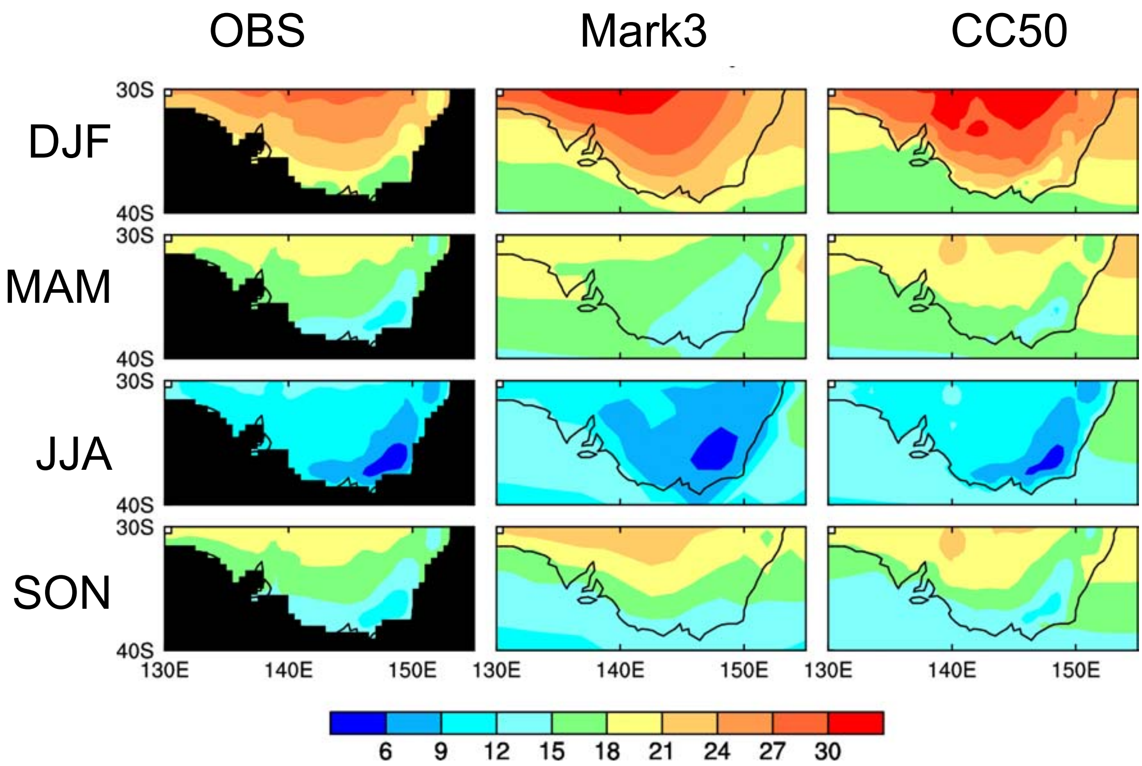

Figure 5. Observed and simulated rainfall patterns by CSIRO Mark3 and CC50. Observed and simulated climatologies are based on years from 1960 to 2000. The left, middle and right columns show observation from the Bureau of Meteorology, Mark3 and CC50 simulations respectively, ordered from top to bottom for DJF, MAM, JJA and SON. Units are in mm.

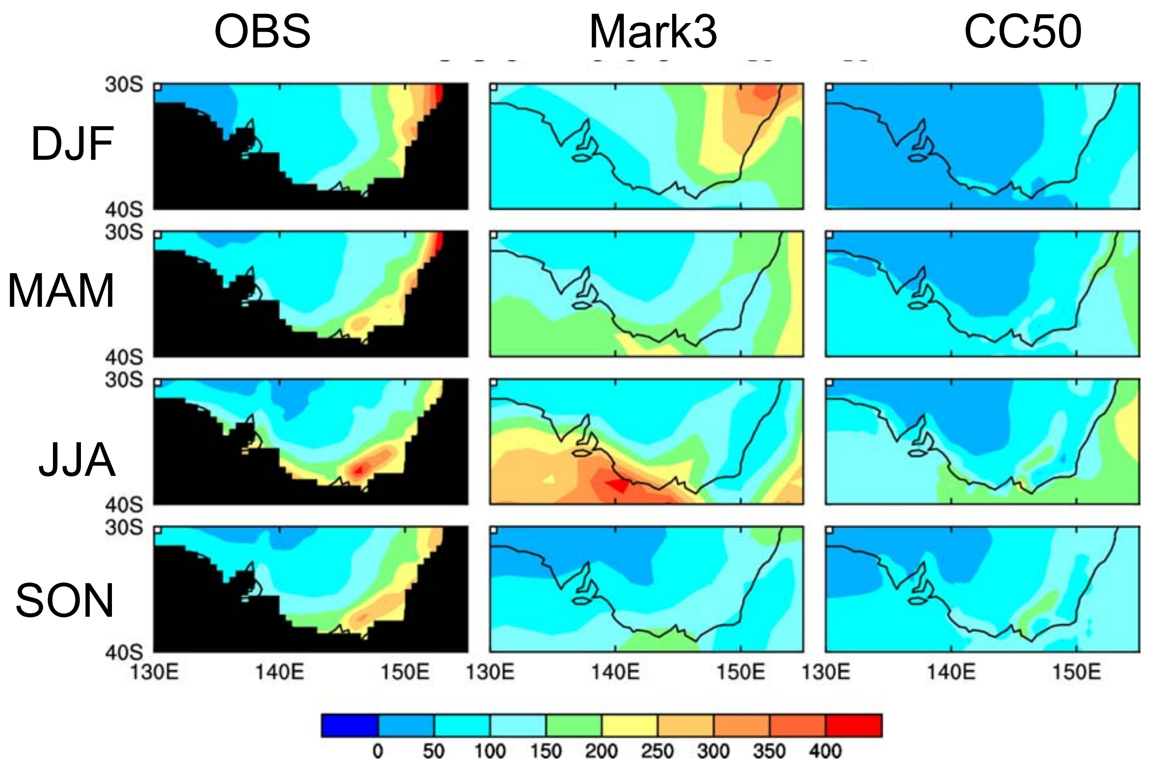

2.2 Patterns of Victorian rainfall variability and associated weather systems: Observations

There is a considerable degree of spatial and temporal variability in Victorian regional rainfall. Trends in seasonal rainfall of southern regions are different to northern regions. In particular, the southwest shows a steady decrease in winter rainfall during the past decade (Whetton *et al*., 2002). To investigate such spatial variations in rainfall, or in other words, to look at the independence of regional rainfall, we have calculated correlations between time series of observed regional rainfall. We have considered annual and seasonal rainfall as there is a strong seasonal dependency in rainfall variability among these regions. The final purpose of this analysis is to see whether the current climate models can simulate regional independence in regional rainfall variability (see next section). If they can, this increases the likelihood that the models can reliably distinguish regional differences in enhanced greenhouse rainfall change over Victoria.

Table 2 shows correlation coefficients between six regions of Victoria. Since seasonal rainfall amounts were calculated using a high resolution data set, and inter-regional correlations tend to show strong differences in correlation values, we have set the correlation threshold value of 0.6 as the cut-off value to represent the independence of rainfall variability of sub regions. In this Table, strong relationships are taken as greater than 0.8 and weak relationships are taken as less than 0.6. In this Table, a weak relationship indicates strong independence of rainfall variability. It is clear from Table 2 that southeast and southwest regions show relatively weak relationships with other regions, and are thus the most independent regions.

Of these, the southeast has the strongest independence in its variability. The southwest region shows a strong relationship with northeast in winter and northwest and north central in spring. Northern regions are strongly correlated in most cases.

The strong spatial variation in regional rainfall fluctuations is caused by the influence of various synoptic systems that affect the State during different seasons and also by the topography of the State. During summer and autumn, the state receives rainfall due to the influence of tropical air masses and such influence is stronger over the northern regions. During winter and spring, Victoria receives its rainfall from mid and high latitude frontal activities. During these seasons, southern regions experience more rainfall compared to northern regions, which get winter and spring rainfall when these fronts penetrate inland. Statewide averaged rainfall variability can show an overall combined influence of various synoptic patterns that affect the State throughout the year. The link between various synoptic patterns and regional-scale rainfall can show the influence of a particular synoptic pattern in a particular season.

Figure 6 shows correlation coefficients between Victoria State-wide rainfall and regional rainfall. There is strong correlation between regional rainfall and state-wide rainfall as the state-wide rainfall is the sum of all regions. Therefore, we have set the cutoff threshold value of correlation as less than 0.8 to distinguish the independence of rainfall variability of sub-regions. As mentioned earlier, weak correlations are associated with strong independence of rainfall variability. From this figure, it is evident that southeast and southwest regions show weak correlations compared to other regions, and hence stronger independence in rainfall variability. The most independent variability occurs in the southeast in all seasons and in annual rainfall, while the southwest shows independent variability in autumn, spring and summer.

Table 2: Correlation coefficients among six regions of Victoria calculated for annual and four seasons using regional rainfall data for 1961-2000. Relatively weak and strong (less than 0.6 and greater than 0.8) correlation coefficients are shown by italics and bold.

ANNUAL

	NW	NC	NE	SW	SC	SE
NW	1.000	**0.931**	**0.875**	0.767	0.778	*0.545*
NC		1.000	**0.953**	0.745	**0.843**	0.645
NE			1.000	0.766	**0.873**	0.723
SW				1.000	**0.886**	0.609
SC					1.000	0.773
SE						1.000

MARCH-MAY

	NW	NC	NE	SW	SC	SE
NW	1.000	**0.916**	0.792	0.724	0.767	*0.554*
NC		1.000	**0.911**	0.637	**0.817**	0.666
NE			1.000	*0.598*	0.772	0.696
SW				1.000	0.784	*0.287*
SC					1.000	0.646
SE						1.000

JUNE-AUGUST

	NW	NC	NE	SW	SC	SE
NW	1.000	**0.938**	**0.821**	0.693	0.727	*0.380*
NC		1.000	**0.887**	0.764	0.784	*0.420*
NE			1.000	**0.817**	0.779	*0.514*
SW				1.000	**0.888**	*0.561*
SC					1.000	0.691
SE						1.000

SEPTEMBER-NOVEMBER

	NW	NC	NE	SW	SC	SE
NW	1.000	**0.926**	**0.818**	**0.822**	0.783	*0.488*
NC		1.000	**0.928**	**0.805**	**0.872**	0.627
NE			1.000	0.748	**0.853**	0.675
SW				1.000	**0.882**	*0.450*
SC					1.000	0.636
SE						1.000

DECEMBER-FEBRUARY

	NW	NC	NE	SW	SC	SE
NW	1.000	**0.893**	0.707	0.670	0.655	*0.382*
NC		1.000	**0.894**	0.676	0.734	*0.550*
NE			1.000	*0.545*	0.606	0.616
SW				1.000	**0.841**	*0.578*
SC					1.000	0.720
SE						1.000

Figure 6. Observed relationships between Victoria statewide rainfall and regional rainfall. Correlation coefficients of less than 0.8 (horizontal line) are highlighted as showing independence of regional rainfall variability.

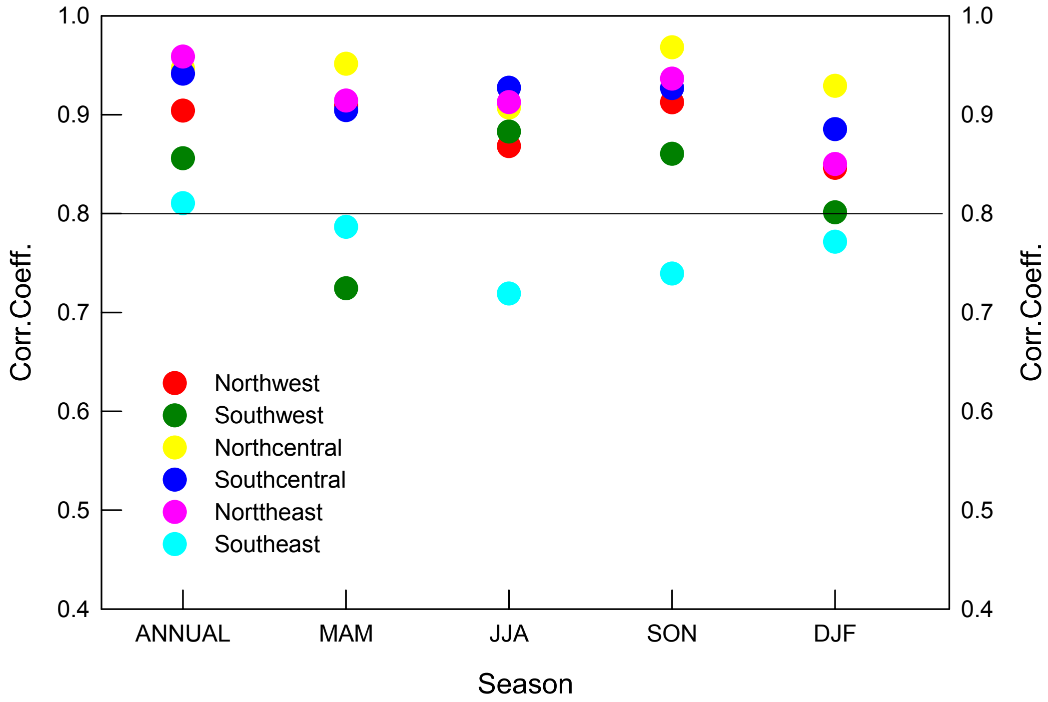

Figure 7 shows monthly correlation coefficients between observed statewide rainfall and mean sea level pressure, which represents the large scale circulation patterns. Strengthening and weakening of correlations show the evolution of the pattern of the relationship between rainfall and mean sea level pressure. In particular, gradual strengthening of the relationship from March to August and gradual weakening from September to February show a strong seasonal dominance of the circulation patterns over Victorian rainfall. Observed relationships between large-scale circulation patterns and state-wide rainfall show that rainfall is strongly correlated with low-pressure systems over southeastern Australia during autumn and winter. During this time, frontal systems associated with low-pressure centres in the mid-latitude westerly regime influence rainfall patterns over Victoria. However, in spring and summer rainfall over Victoria is linked to a broader low- pressure region over the continent. A notable feature during summer is the high- pressure system over the Tasman Sea that enhances rainfall over Victoria, particularly in the eastern part.

We also calculated correlations between regional rainfall and mean sea level pressure on a seasonal basis. The results are shown in Figures 8 and 9. In general, southern regions show stronger correlations during autumn and winter compared to northern regions. The southwest shows the strongest link during winter. However, southeast, north-central and northeast regions indicate strong relationship with the high pressure system over Tasman Sea.

2.3 Patterns of Victorian rainfall variability and associated weather systems: Current climate models

The analysis presented in the last section was using the climate model outputs and comparison with the observational results made.

Annual and seasonal values of simulated data from 1961 to 2000 have been used to see whether global and regional climate models simulate the spatial variations of rainfall among six regions. Since different climate models have different horizontal resolutions, we have interpolated simulated rainfall results from coarse resolutions to a finer 60 km grid over southeastern Australia, that enables the demarcation of the Victorian regions precisely. Figures 10 to 13 show correlation coefficients between state-wide rainfall and regional rainfall based on annual and seasonal values. In these figures, results from twelve climate model experiments are shown and compared with the observed results (also given in figure 6). A correlation coefficient of 0.8 was chosen in these figures as a threshold value to assess the model performance in simulating regional difference in rainfall variability (see Table 3). As observed, the southeast region shows correlation coefficients of less than 0.8 in all seasons, while the southwest shows this during autumn and about 0.8 during summer. On the other hand, stronger relationships (greater than 0.8) in other seasons and other regions are indicative of strong interregional coherence in regional rainfall variations. On the whole, the models are able to simulate the greater independence of rainfall variations in the southeast and southwest compared to other regions of the State. This feature is best developed in the CCCM1, HADCM3, ECHAM4, CCCM2, Mark3 simulations, and in particular in the higher resolution DAR125, DAR60 and CC50 simulations. This is an encouraging result. It suggests that inter-regional differences in simulated future changes in rainfall may be realistically simulated in current climate models, and that providing future rainfall projections at this scale is justifiable on these grounds.

Figure 7. Observed relationships between Victoria State-wide rainfall and mean sea level pressure.

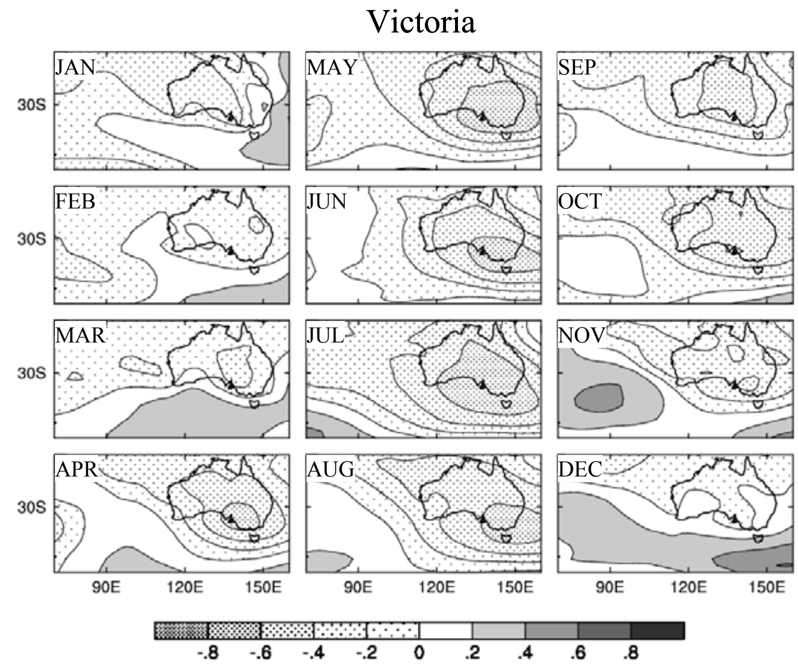

Figure 8. Observed relationships between northern regions rainfall and mean sea level pressure.

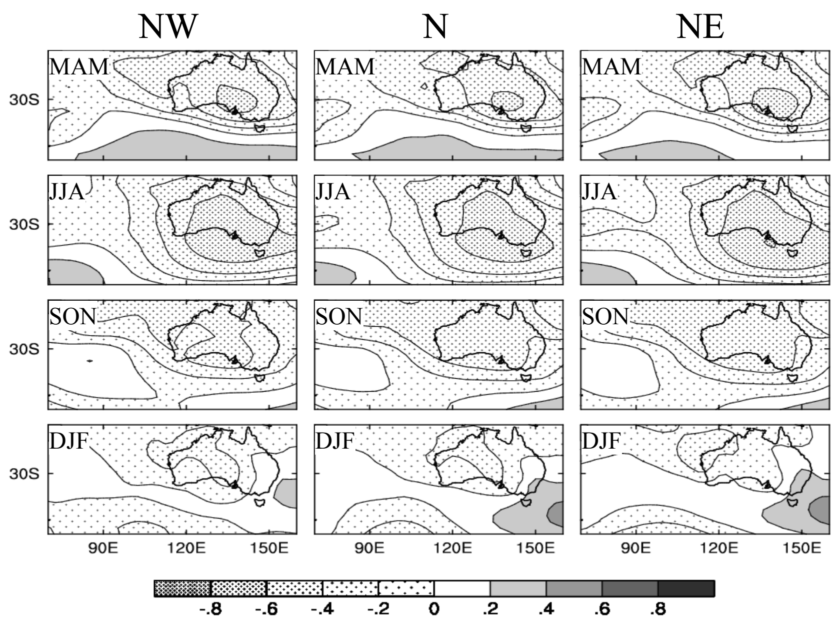

Figure 9. Observed relationships between southern regions rainfall and mean sea level pressure.

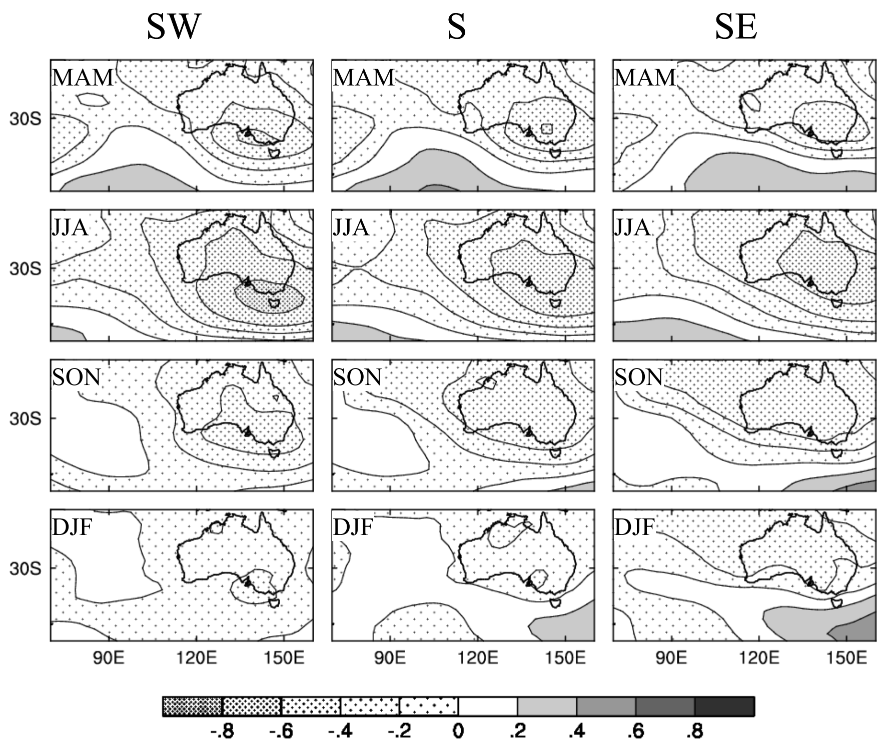

Figure 10. Correlation coefficients between statewide rainfall and regional rainfall for CCCM1, HADCM2 and HADCM3. ANN1, MAM1, JJA1, SON1 and DJF1 indicate values based on model results for annual, autumn, winter, spring and summer, respectively. ANN), MAMO, JJAO,SONO and DJFO show correlations based on observation.

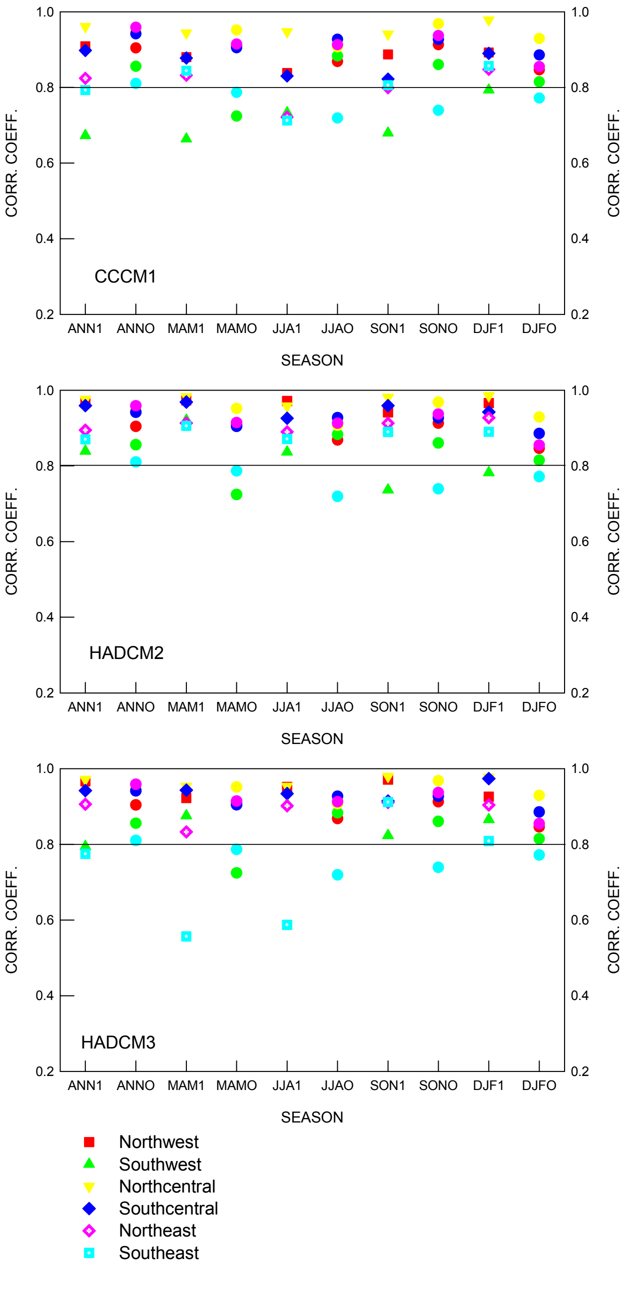

Figure 11. Same as in Figure 10, but for ECHAM3, ECHAM4 and GFDL.

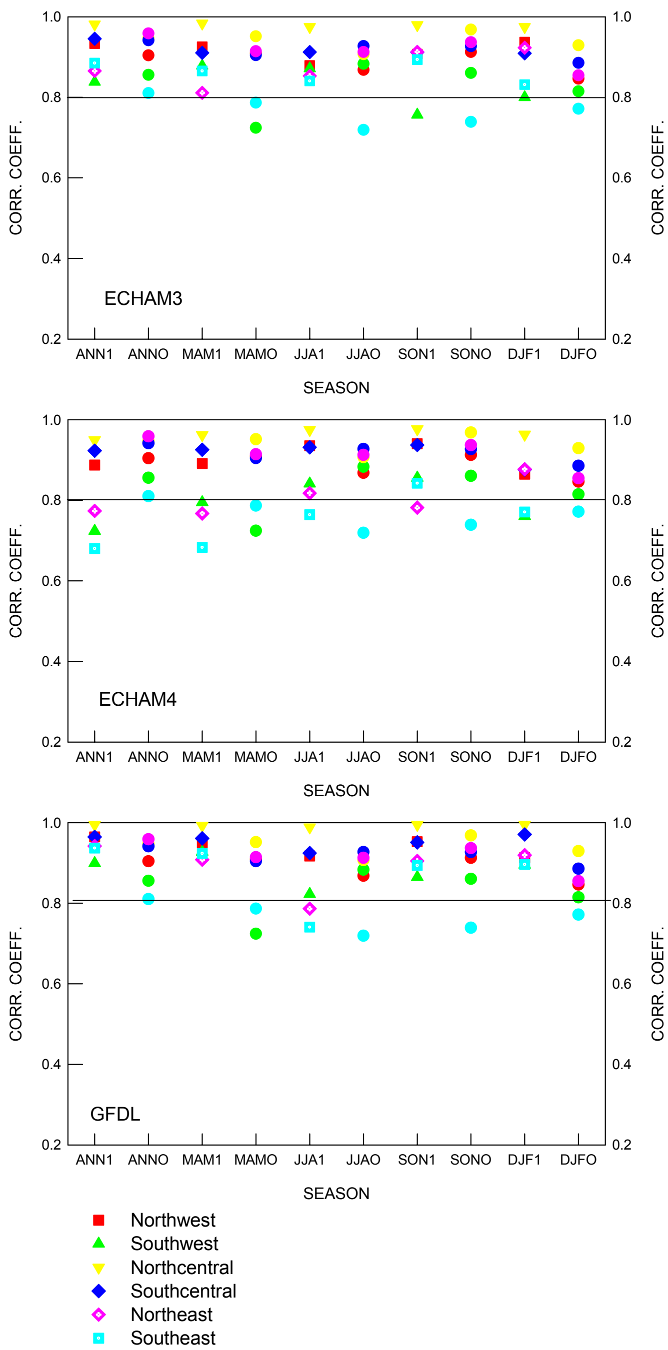

Figure 12. Same as in Figure 10, but for CCCM2, Mark2 and Mark3.

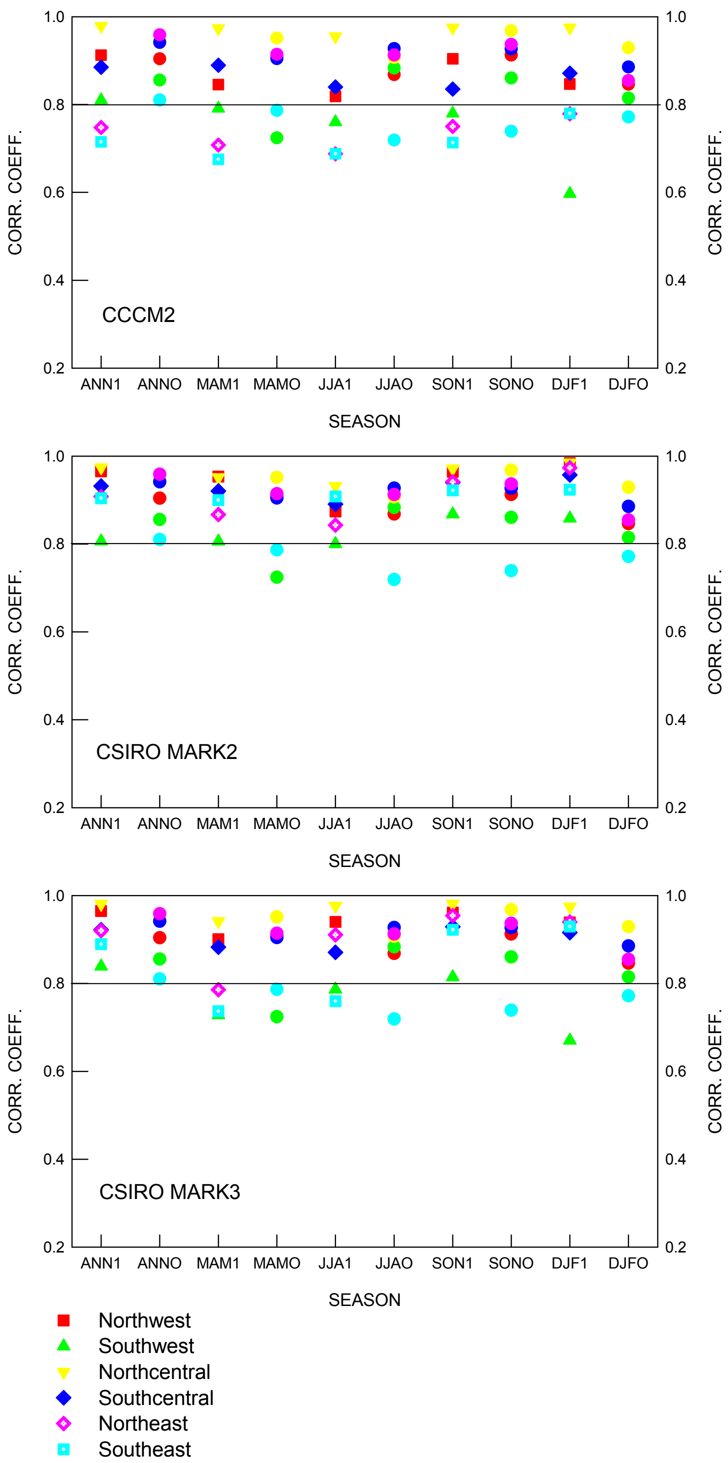

Figure 13. Same as in Figure 10, but for DAR125, DAR60 and CC50.

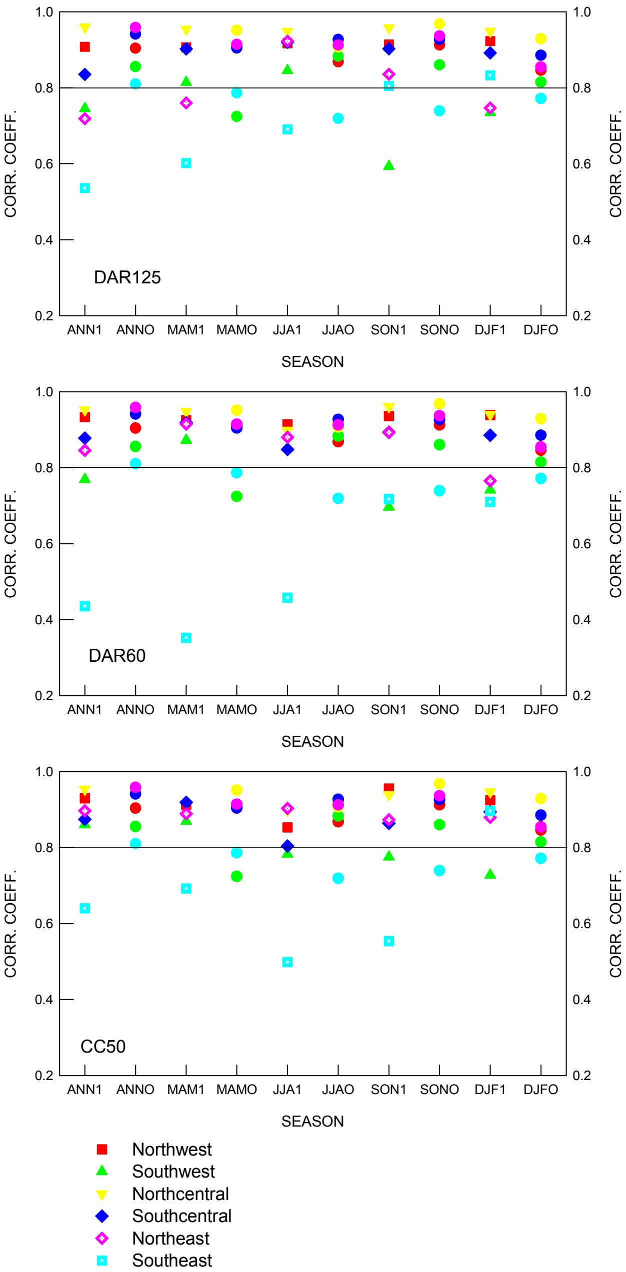

Table 3. Inter-regional correlation of rainfall variations: model versus observations. A dot indicates a correlation of regional rainfall with state rainfall of less than 0.8 and a cross more than 0.8. Dots thus indicate regions and seasons where region rainfall anomalies show greater independence of statewide anomalies. Seasons are autumn (A), winter (W), spring (S) and summer (S). Northwest and northcentral regions (not shown) show crosses for all cases.

Model	**Southeast**	**Southwest**	**Northeast**	**Southcentral**
Seasons	A W S S	A W S S	A W S S	A W S S
CCCM1	× ● ● ×	● ● ● ●	× × ● ×	× × × ×
HADCM2	× × × ×	× × ● ●	× × × ×	× × × ×
HADCM3	● ● × ●	× × ● ×	× × × ×	× × × ×
ECHAM3	× × × ×	× × ● ●	× × × ×	× × × ×
ECHAM4	● ● × ●	● × × ●	● ● ● ×	× × × ×
GFDL	× ● × ×	× ● × ×	× ● × ×	× × × ×
CCCM2	● ● ● ●	● ● ● ●	● ● ● ●	× × × ×
MARK2	× × × ×	● ● × ×	× × × ×	× × × ×
MARK3	● ● × ×	● ● ● ●	× ● ●●	× × × ×
DAR125	● ● ● ×	● × ● ●	● × × ●	× × × ×
DAR60	● ● ● ●	× × ● ●	× × × ●	× × × ×
CC50	● ● ● ×	× ● ● ●	× × × ×	× ● × ×
OBSERVATION	● ● ● ●	● × × ●	× × × ×	× × × ×

We now consider the correlation between Victorian rainfall and mean sea level pressure anomalies using the model data. Detailed results are presented for the state and for the more independent sub-regions of Southeast and the Southwest.
The maps we then obtained represent the equivalent for the models of the observed maps presented for regions in Figures 7 and 8 (and for the state as a whole as presented in figure 15 from last year's report (Whetton *et al*., 2002)). Then to assist in the comparison of the model and observed patterns in these maps, pattern correlations have been calculated. Since this a fairly severe test to assess model performances, we have set the threshold value of 0.4 to identify models that adequately simulated the seasonal link between rainfall and pressure anomalies under control climate. The results are shown in Table 4. Most of the models simulate the pressure-rainfall relationship during winter and to a lesser extent in autumn. Performance is poor in spring, and particularly so in summer.

Table 4. Global and regional climate models ability to simulate the relationship between large-scale circulation patterns and rainfall over Victoria as a whole and also for subregions of Southeast and Southwest. The capability of the models of simulating the relationship is determined by a threshold value of pattern correlation of 0.4. Dots indicate values greater than 0.4 and crosses less than 0.4. Seasonal results for autumn (A), winter (W), spring (S) and summer (S).

Model	Southeast	Southwest	Victoria
Seasons	A W S S	A W S S	A W S S
CCCM1	× × × ×	● × ● ×	× × × ×
HADCM2	× × × ×	● ● ● ×	× × × ×
HADCM3	× ● × ×	× ● × ×	× ● × ×
ECHAM3	× ● × ×	● ● ● ×	× ● × ×
ECHAM4	× ● × ×	● ● × ×	× ● × ×
GFDL	● ● × ●	● ● ● ●	● ● ● ×
CCCM2	× ● × ●	● ● × ×	● ● × ×
CCCM3	× ● × ×	● ● × ×	× ● × ×
MARK2	● ● × ×	● ● × ×	● ● × ×
MARK3	● ● × ×	× ● ● ×	● ● × ●
DAR125	× ● × ×	● ● × ●	× ● × ×
CC50	× ● × ×	● × ● ●	× × × ×

2.4 Assessment of simulated present-day climate of Victoria by climate models

Almost all the models simulate average patterns of observed temperature and sea level pressure realistically. However, there is a strong variation among the models in simulating the present-day rainfall pattern and the link between rainfall and atmospheric circulation patterns. All models show a mix of good features and poor features. No model or group of models stand out as clearly poorer than the rest. However, the high resolution simulations (e.g DAR60 and CC50) do tend perform a little better than the other models. It is also notable that where we have newer and older simulations from the same modelling group (e.g. CSIRO Mark3 and Mark 2, CCM2 and CCM1), the newer simulations usually perform better. Therefore, at this stage, we have decided to include all available models to produce revised climate change projections for Victoria (see section 4), although we only use DAR60 of the closely related DAR60 and DAR125 simulations. However, in section 4 we also examine the effect of leaving out the older simulations where more than one was available from a modelling group, but this did not have a significant impact on the results.

However, the analysis presented in this chapter has revealed some very valuable information which bears upon our assessment of the reliability of climate change projections of rainfall over Victoria using current models. First, it has been shown that most current models can distinguish different regions of the state in terms of independence in their current rainfall variability. This gives significant additional justification for providing regional detail in simulated rainfall change over Victoira using current models. Second, we have shown that that rainfall-producing processes (as indicated by the link between rainfall anomalies ands pressure anomalies) are reasonably well simulated in winter and autumn, but less well simulated in spring and summer. In this light, the spring and summer projected rainfall changes should be viewed as less reliable. This is considered further where the current projections are presented later in report.

2.5 Mean sea level pressure changes under enhanced greenhouse conditions

Here we consider the simulated change in atmospheric circulation under enhanced greenhouse conditions. Our assessment of the reliability of simulated changes in rainfall, in particular, will be affected by the realism of the changes in circulation with which the rainfall changes are associated.

Since most of the models capture the link between rainfall and pressure, particularly during autumn and winter, we have constructed pressure anomalies between 40 year periods of simulations of all available models. The anomalies are taken as the difference between the average of the last 40 years and the average of the first 40 years. Figure 14 shows seasonal and annual pressure differences between two 40-year periods. The annual values show decreases over the continent and increases over the southern ocean. There are considerable variations between the seasons. In summer, pressure decreases dominate most of the continent and the decrease is stronger over southeastern Australia. However, during other seasons, there is a tendency for an increase in pressure over southern ocean and slight decrease in pressure over the continent. Increases in pressure south of the continent would lead to weaker westerlies, and hence, weaker frontal systems that could result in decreases in rainfall over most of southern Australia.

Pressure differences shown in Figure 14 indicate a gross picture, which is based on a number of models, but there is strong model-to-model variation in the pressure difference between the two 40-year periods. As stated earlier, not a single model stands out in clearly representing the link between rainfall and circulation patterns in all seasons. Therefore, decreased rainfall over Victoria under enhanced greenhouse conditions could be partially explained by the composite analysis of pressure anomalies at this stage. Further analysis on the processes that cause dry or wet conditions are needed when climate models can simulate the link between rainfall and circulation during all seasons.

Figure 14. Mean sea level pressure difference between first 40 years and the last 40 years of simulations. Simulations from all available models are used as there is not a single models stands out clearly as best simulating the link between rainfall and circulation patterns.

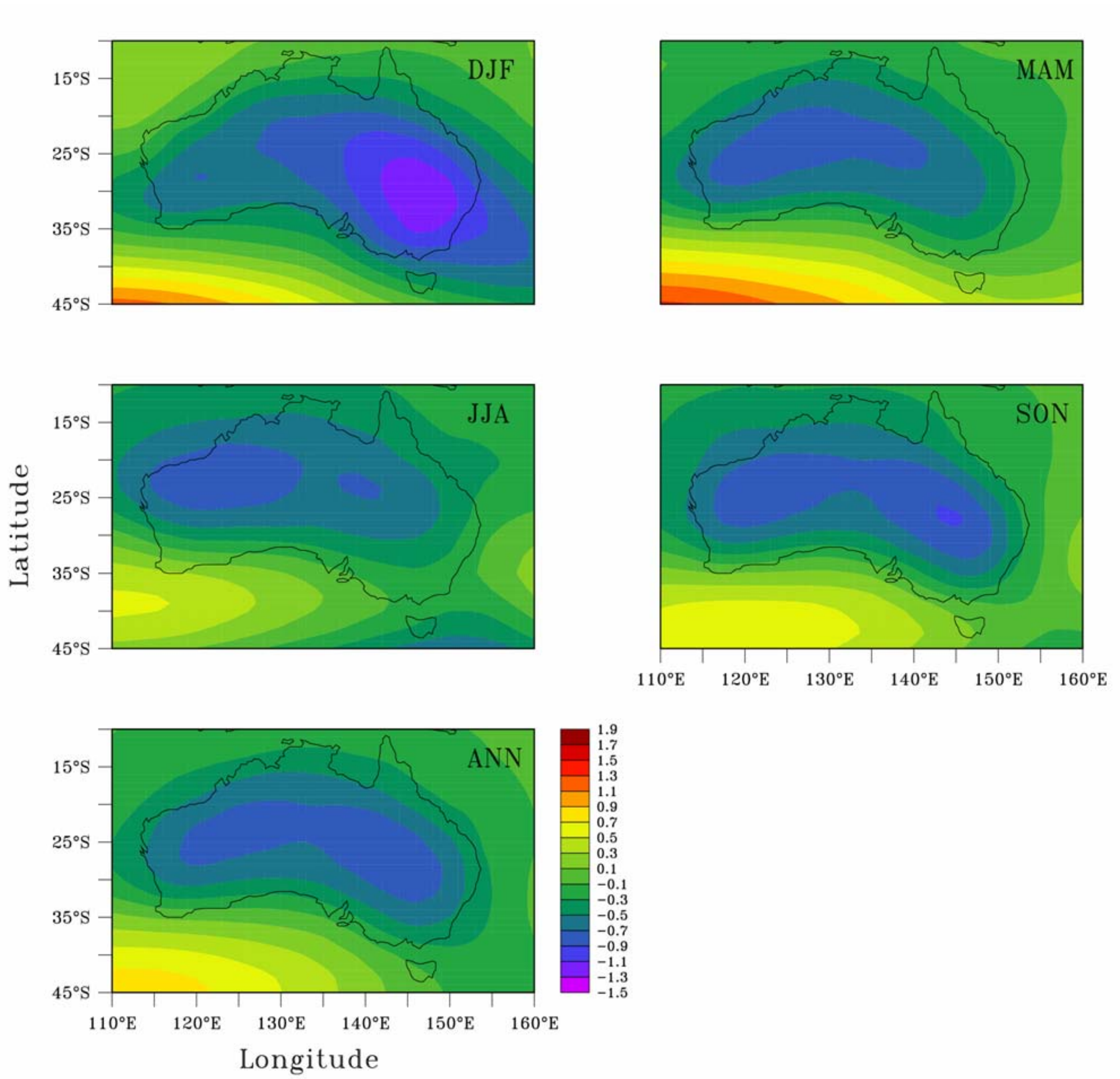

3 Extreme Rainfall Events: A Further Analysis

A number of studies showed that extreme daily rainfall over Victorian regions generally increased with global warming. The latest Victorian report (Whetton *et al*., 2002) also suggested that changes in extremes may relate to those in means. Indeed some relationship can be anticipated from recent studies of theoretical models of rainfall. If the change in extreme rainfall can be consistently related to the change in mean rainfall, this would assist greatly in the development of projected changes in extreme rainfall for use in impact studies. The new work presented here explores these ideas. We also consider the possibility of using the variability of monthly means, which is more commonly available in data archives than is daily data, to infer extremes.

A basic difficulty of studying extremes over climatic periods is the need for multiple simulations in order that statistically significant changes can be determined. Two new five-member ensembles of simulations by the CSIRO Mark 2 coupled model are thus considered. In this low-resolution model Victoria is largely covered by only two model grid squares, 'East and West Victoria'. Nevertheless, there are differences in the weather patterns associated with rainfall in the two, as can be inferred from the previous section of this report. Adjacent squares in the Australian maps that will be presented are also of interest, particularly for the north-west of the state and coastal regions.

3.1 Simulations of rainfall change

One of the ensembles represents the greenhouse gases, sulphate and ozone forcing of climate over the period 1871-2100, with the SRES B2 scenario used into the future. The other represents the change beyond 1990 under the A2 scenario, which has larger greenhouse gas (GHG) concentrations. Averaging over the five members in each case produces a smooth global mean warming trend (see Watterson and Dix, 2002, for details), with a mean warming from the period 1871-1900 to 1961-1990 of 0.3ºC. While the greater sulphate loading in A2 results in its global warming being a little smaller than for B2 in the near future, this is later overcome by the GHG forcing. We focus on the change from 1961-1990 to 2071-2100, with the A2 mean warming being 3.5ºC, and the B2 warming 2.7ºC. The two spatial warming patterns are very similar, so we consider only the larger A2 case. Global mean precipitation P increases 6.3%. In general, it seems justified to maintain the usual practice of assuming that regional changes in rainfall, including extremes, are linear in the global mean warming.

Percentage changes in precipitation in the four seasons (again, the differences between the averages over the five simulations) are shown for the Australian region in Figure 15. Decreases predominate, with the eight Victorian values ranging from –3% to –23%, the largest loss being in spring. The 90% confidence ranges, based on variation among the ensemble members, are about ±7%. Thus significant decreases, but no increases, are indicated in these cases. Some seasonal increases in the west and north of Australia are offset in the annual result by decreases in other seasons, as will be shown shortly.

Figure 15. Percentage change in seasonal averages of daily rainfall, from 1961-1990 to 2071-2100 in the CSIRO Mark 2 model (A2): (a) December-February, (b) March-May, (c) June-August, and (d) September-November.

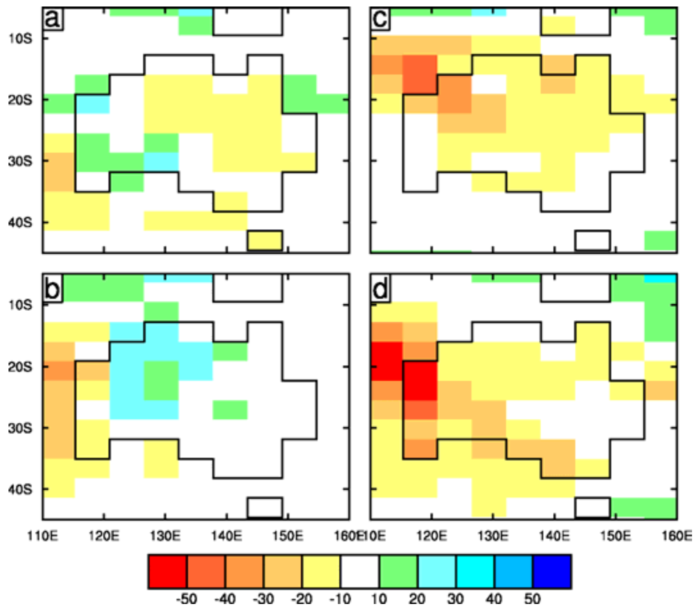

3.2 Daily extremes of rainfall

Daily precipitation amounts have been further examined for the two targeted 30-year periods, with monthly stratification. Combining values from the five simulations provides highly resolved frequency distributions, as in the East Victoria January case shown in Figure 16. Among 'wet' days, very light rain is common, but values as high as 40 mm are recorded. Naturally, as these represent averages over the large area of a grid square, the values are much lower than extremes observed at points. A good match to the distribution is provided by the gamma distribution, which requires only two parameters, 'scale' and 'shape', determined from the mean and variance (the 'method of moments'; Watterson and Dix, 2003).

Figure 16. Frequency of daily precipitation at the East Victoria grid point, for January days during 1961-1990. Data from five simulations are combined to produce a histogram with bar width 0.1 mm. The dry day frequency, 0.6, is not depicted, as are daily values from 20 mm to the extreme value 40.5 mm. The gamma distribution fitted to the data is shown as a line.

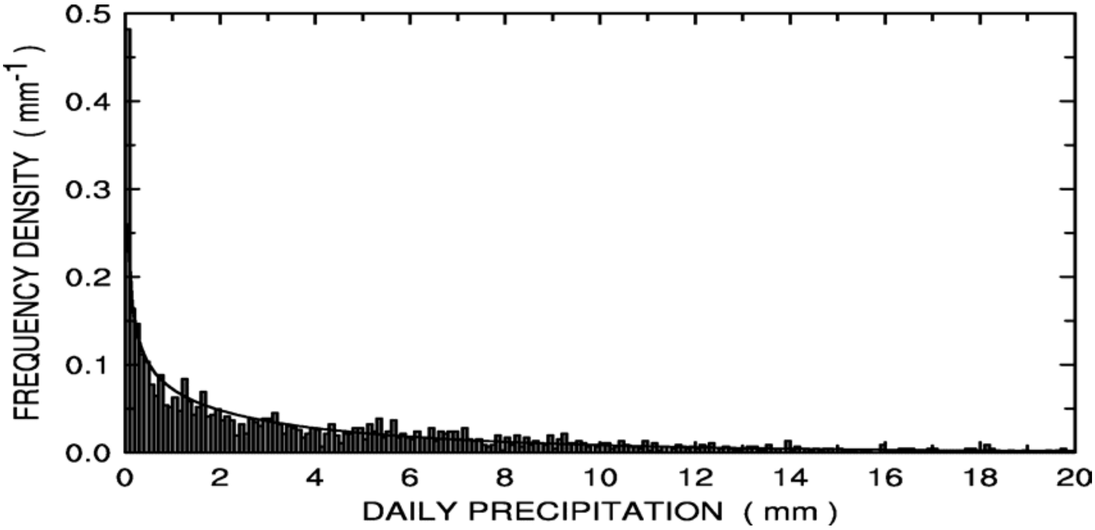

The extreme value in each case, a 30-month extreme, was extracted, and the average and standard deviation of these over the five simulations was determined. To further improve significance, these have been further averaged over the three months from each season, providing an effective 10-year extreme for each season (hence matching those depicted in the 2002 report). Percentage changes from 1961-1990 to 2071-2100 over Australia are shown in Figure 17. Little change occurs over some squares and seasons, but increases are also common. For the Victorian squares values range from –6% to +25%. Unfortunately, the 90% confidence ranges for the differences are still typically ±14%. A general increase is clear, nevertheless, and there is a significant seasonal contrast, with the western values increasing in autumn-winter, and the east increasing in spring-summer.

Figure 17. Percentage change in seasonal averages of 30-month extremes of daily rainfall (effectively 10-year extremes), from 1961-1990 to 2071-2100 (A2): (a) December-February, (b) March-May, (c) June-August, and (d) September-November.

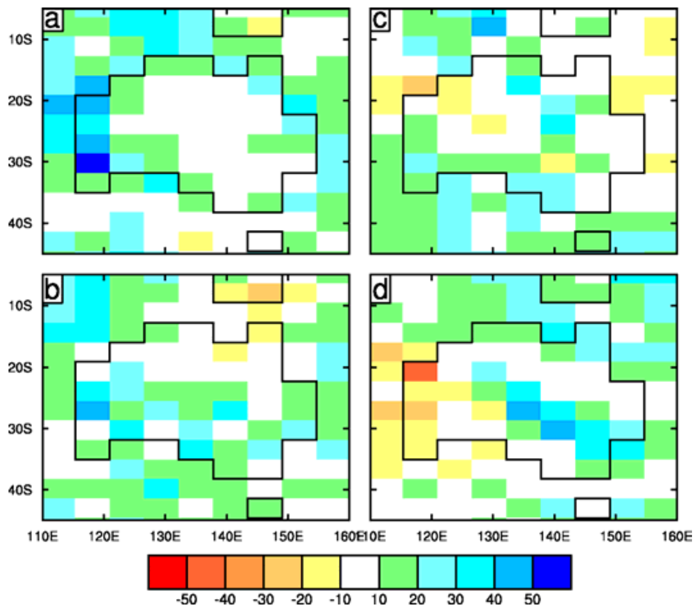

Annual mean changes in rainfall for the Australian region are shown in Figure 18a. Most grid squares, including East and West Victoria, show a decrease. Taking the extreme of the twelve monthly extreme fields produces a true 30-year extreme of daily rainfall. The difference of these is shown as a percentage in Figure 18b. Increases predominate, the largest occurring in the west. Victorian increases are considerable.

Figure 18. Percentage change in (a) annual mean rainfall and (b) 30-year extremes of daily rainfall, from 1961-1990 to 2071-2100 (A2).

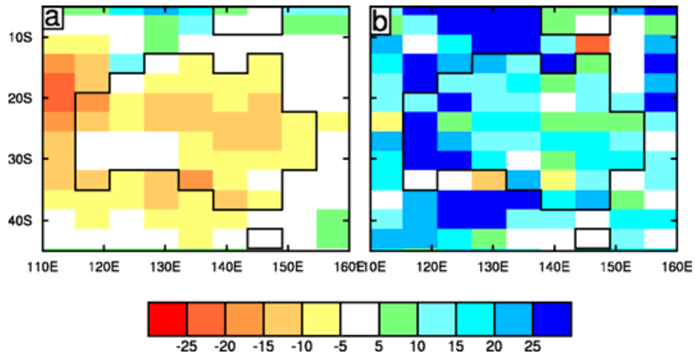

It is clear that changes in the extremes are more positive than those in the means, indeed often of the opposite sign over Australia. Nevertheless there is some link between the percentage change fields, for example, in the seasonal variation in the means and extremes on the west coast of Australia (comparing Figures 15 and 17). The spatial correlation between the fields over Australia (restricted to squares with a mean of > 0.5 mm d^{-1}. ranges from –0.1 to 0.7, over the seasons. Globally the correlations are around 0.6. However, for Victoria there seems little link, given the scatter of the seasonal and annual changes depicted in Figure 19a .

Figure 19. Percentage changes in extreme rainfall for the East and West Victoria grid points, plotted against percentages changes in the (a) mean, and (b) the ratio of variance to mean. Values for the four seasons are shown as dots, and the annual values, for the (a) case, are shown as stars.

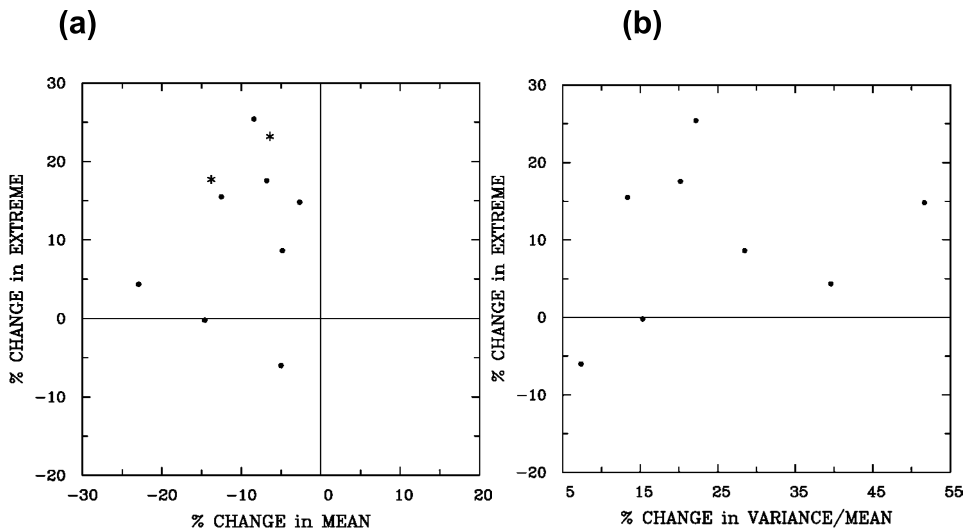

3.3 Extreme value relationships inferred from theory

Katz (1999) applied extreme value theory to the daily rainfall modelled by a combining the gamma distribution for amounts with a simple chain model for the sequence of wet and dry days (of which the frequency of wet days is the key parameter). Watterson and Dix (2003) showed that the theory worked remarkably well for much of the globe, when applied with monthly stratification. For example, the expected 30-month extreme in the East Victoria, January case of Figure 17 is close to the actual values, even though the gamma distribution is based on all the wet days, not just the extremes. The percentage changes due to global warming in the extreme values are also well matched by the theory. Note, though, that this still relies on parameters for the changed climate determined from all the GCM data.

In this theory, changes in the extremes are most strongly influenced, indeed linearly, by changes in the scale parameter of the gamma distribution. For example, the percentage changes in the East Victoria point, averaged over DJF, are around 14% for both the extremes and the scale parameter, and around 15% for both in SON. Agreement in other seasons is less close, possibly due to sampling. Globally averaged, and excluding very dry squares, the scale parameter increases 17%, compared to 13% for the 30-month extremes, as decreases in the frequency of wet days, and the shape parameter tend to reduce the extremes. Since the mean rain is equal to the product of the three parameters it is also varies with the scale parameter, providing a link between extremes and the mean precipitation. This is degraded by changes in the frequency and shape, however, leading to the relatively small global mean increase in precipitation (6.3%).

Watterson (2003) also applied the statistical model to the problem of interannual variability of monthly means. While the model tends to underestimate this variability, particularly in the tropics, the changes in the statistical model's variability are nevertheless strongly influenced by the scale parameter. In particular, the ratio V/P, where V is the variance of monthly means (of all Januarys, for instance) and P the mean precipitation, is proportional to the scale parameter. Globally, V/P increases some 14-19%, similar to both the scale and extreme changes. The field is typically well correlated (0.7) with those in the scale parameter. However, the correlation with the extremes is around 0.5 in each season. The set of 8 results for Victoria is shown in Fig. 19b. The match between changes in V/P and the extremes does seem closer for Victoria than that between P and the extremes.

This theoretical result would be useful as a basis for inferring changes in daily extremes for other GCM simulations, for which there is only monthly data. One might use as an estimation for the percentage change in such extremes, the changes in the V/P ratio, either local or area-averaged values. To be able to do this would enable us to build in model to model variations into our projected regional extreme rainfall change – this is a key uncertainty that is not well represented at present. The ratio V/P in itself is of interest, and may have further applications to water resource management.

4 Revised Climate Change Scenarios for Victoria

In this section we present revised maps showing projected changes in rainfall for Victoria. These have been constructed in the same manner as those presented in last year's report, except that two different sets of climate model simulations have been considered. First we have added three additional models (CSIRO Mark 3, the high resolution CC50 and the latest Canadian Climate Center simulation, CCM2) to the nine models used last year, to create a set of twelve simulations. We then considered a new set of nine simulations (an 'optimal set') by deleting three simulations which may be considered as superceded by later simulations from the same modeling group (HadCM2, CCM1, and CSIRO Mark 2 were deleted).

As in last year's report, we present ranges of change in temperature and precipitation, which incorporate quantifiable uncertainties associated with the range of future emission scenarios, the range of global responses of climate models, and model to model differences in the regional pattern of climate change.

The ranges are based on:

- the full range of IPCC global warming projections, which provide information on the magnitude of the global climate response over time. These ranges take into account a range of possible future emissions of greenhouse gases as well as uncertainty associated the sensitivity of the climate system.

- the regional response in terms of local change per degree of global warming. A range of local values is derived from the differing results of set of climate model simulations.

Figure 20. Pattern of annual and seasons warming from an optimal set of nine models (left panels) and from all available twelve models (right panels). Units: Degrees C. Model details are given in Table 1.

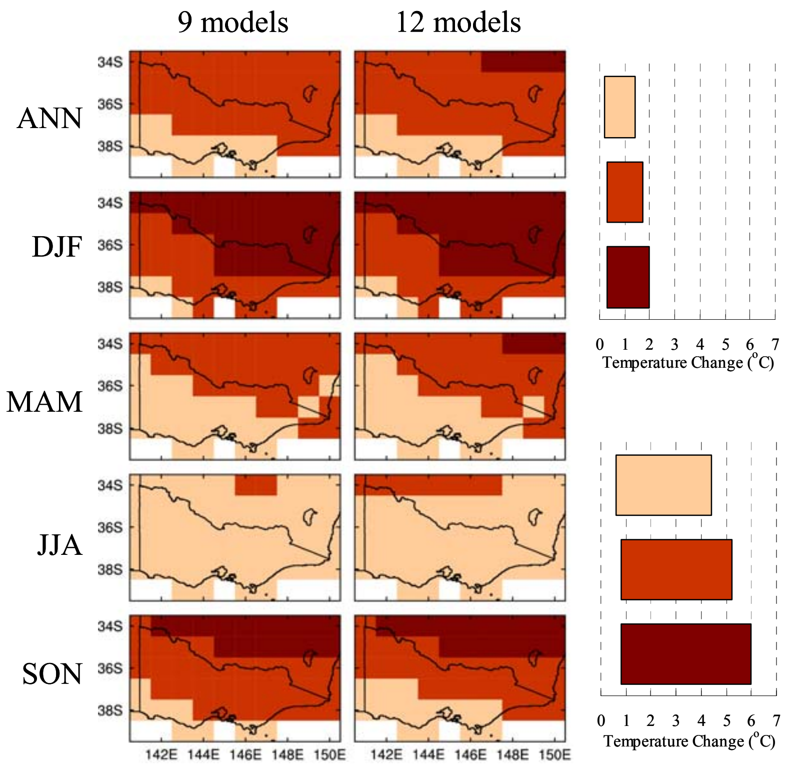

4.1 Average temperature changes

Spatial results are presented in Figure 20 as colour-coded maps for changes in average temperature by around 2030 and 2070 relative to 1990. These selected dates illustrate changes in average temperature that may be expected in the next few decades and the larger changes that may occur late in the century. The changes in temperature given for these dates represent the change in average temperature conditions. The conditions of any individual year will continue to be strongly affected by natural climatic variability, which cannot be easily predicted.

Annual average temperatures over the north and east of the State are projected to be between 0.3 and 1.6^{o}C higher by 2030 and between 0.8 and 5.0^{o}C higher by 2070, relative to 1990. In the south, the ranges are 0.2 - 1.4^{o}C by 2030 and 0.7 - 4.3^{o}C by 2070. The warming is projected to be greatest in summer and least in winter. Differences between the patterns form the two sets of models are not significant. Results from either set are also very similar to the warming patterns presented in last years report. There is, however, a slight tendency in the new results for greater warming in northern Victoria in autumn.

4.2 Regional average rainfall changes

Figure 21 shows ranges of change in Victorian rainfall for around 2030 and 2070. Projected annual average rainfall ranges tend toward decrease over most of the state (–15% to +3% in 2030 and –40% to +10% in 2070 in the north, and –9% to +3% in 2030 and–25% to +9% in 2070 in the south).

In summer, northcentral and northwestern part parts of the State shows increases and decreases in the range of –15 to +15% by 2030 and in the range of –40 and +40 by 2070. In other areas, projected summer ranges tend towards decreases which range between -10 to +5% by 2030 and between –40 and +20 by 2070. Autumn shows changes ranging between –10 and +10% by 2030 and –25 and +25% by 2070 over northwest, northcentral and eastern parts of Victoria. The other regions show changes between –10 and +5% by 2030 and –20 and +10% by 2070. In winter, rainfall changes over most of the state range between –10 and +5% by 2030 and between –25 and 10% by 2070. In spring, almost all of the state shows decreases. Decreases range between –20 and –2% by 2030 and between –60 and –5% by 2070. However, the eastern part of the state shows less decrease than other parts of the state.

Figure 21. Annual and seasonal rainfall changes (in percentage) for Victoria from an optimal set of nine models (left panels) and from all available twelve models (right panels). Model details are given in Table 1.

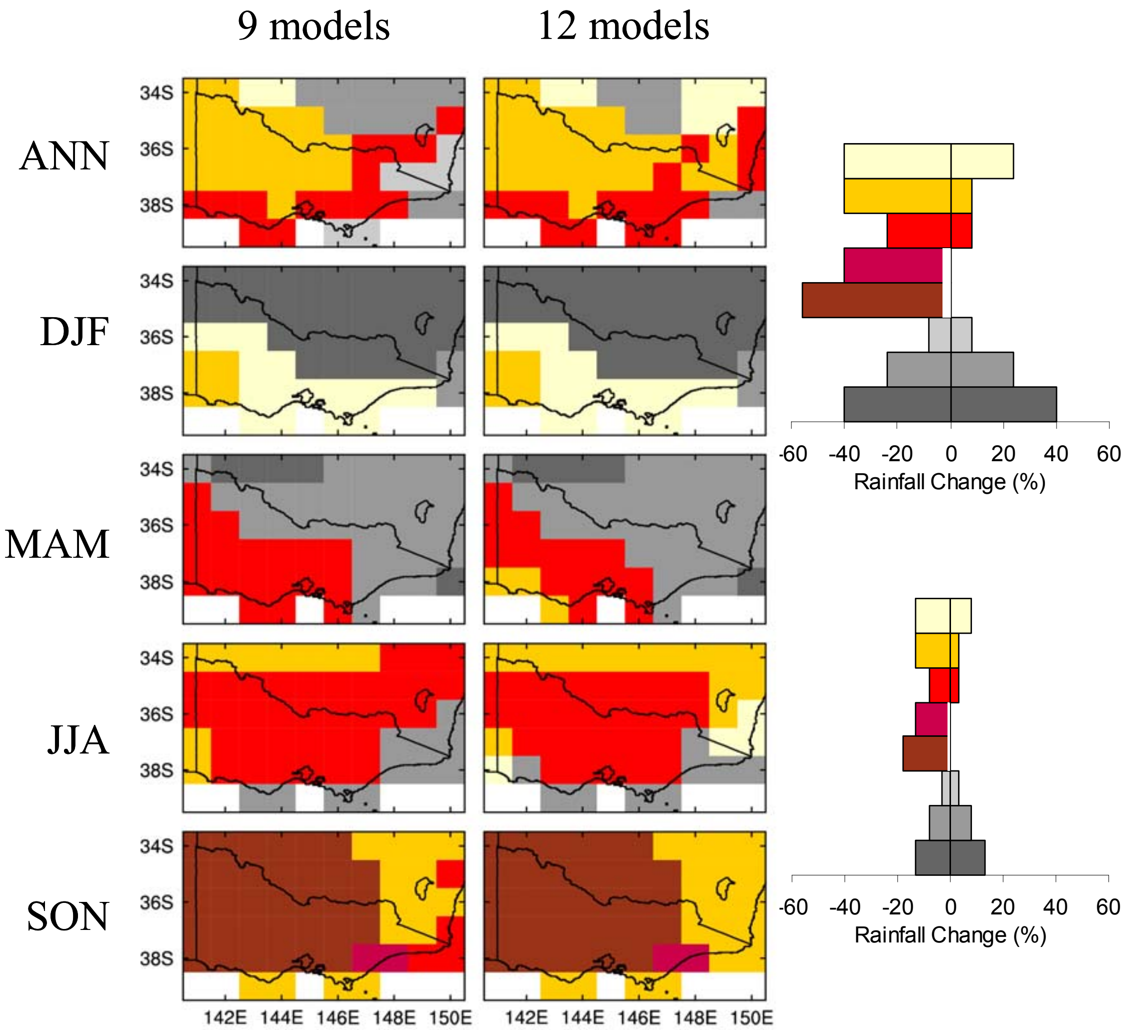

Differences between the patterns from the two sets of models are not significant. Results from either set are quite similar to the rainfall change projections presented in last years report. There is, however, a tendency in the new results for greater rainfall decrease in spring, with this then contributing to a stronger annual rainfall decrease. However, given that in this report we have also found that rainfall-bringing processes are not as well simulated by current models in spring as they are in autumn and winter, the change in the spring projections should not necessarily be viewed as significant.

5 Conclusions

Revised climate change scenarios for temperature and rainfall changes for Victoria do not significantly differ from the previous climate change scenarios. Annual average temperatures over the north and east of the State are projected to be between 0.3 and 1.6°C higher by 2030 and between 0.8 and 5.0°C higher by 2070, relative to 1990. In the south, the ranges are 0.2 - 1.4°C by 2030 and 0.7 - 4.3°C by 2070. The warming is projected to be greatest in summer and least in winter.

Projected annual average rainfall ranges tend toward decrease over most of the state (–15% to +3% in 2030 and –40% to +10% in 2070 in the north, and –9% to +3% in 2030 and–25% to +9% in 2070 in the south). The decreases are strongest in spring through most of the State. On the other hand, over northern Victoria in summer and autumn and over parts of southern Victoria in winter, the direction of rainfall change is uncertain.

The analysis presented in this report has shown that most current models can distinguish different regions of the state in terms of independence in their current rainfall variability. This gives significant additional justification for providing regional detail in simulated rainfall change over Victoria using current models. The potential realism of simulated differences in rainfall change in, say, northern versus southern Victoria, has been enhanced.

The link between seasonal rainfall over Victoria and mean sea level pressure over a broad region that encompasses parts of the Indian and southern oceans and the Australian continent indicates that most of the models simulate observed spatial patterns of correlation during autumn and winter, but only a few models capture the relationship during spring and summer. In this light, the spring and summer projected rainfall changes should be viewed as less reliable, and autumn and winter changes as more reliable.

An analysis of extreme rainfall from CSIRO Mark2 indicates an increase in extreme rainfall under enhanced greenhouse conditions. More significantly, the analysis has indicated that it likely to be possible to estimate changes in daily extreme rainfall from changes in monthly mean and standard deviation. To be able to do this would enable us to build in model to model variations into our projected regional extreme rainfall change – this is a key uncertainty that is not well represented at present.

6 References

Gordon, H. B., Rotstayn, L. D., McGregor, J. L., Dix, M. R., Kowalczyk, E. A., O'Farrell, S. P., Waterman, L. J., Hirst, A. C., Wilson, S. G., Collier, M. A., Watterson, I. G. and Elliott, T. I. 2002. *The CSIRO Mk3 Climate System Model.* CSIRO Atmospheric Research Technical Paper No. 60. CSIRO, Aspendale.

IPCC, 2001. *Climate Change: Scientific basis of climate change*, Summary for policymakers. Intergovernmental Panel on Climate Change, Cambridge University Press, 98p.

Katz, R. W.1999. Extreme value theory for precipitation: sensitivity analysis for climate change. *Adv. in Water Resources,* 23*,* 133-139.

McGregor, J. L., Nguyen, K. C., and Katzfey, J. J. 2002. Regional climate simulations using a stretched-grid global model. In: Research activities in atmospheric and oceanic modelling. H. Ritchie (ed.). (CAS/JSC Working Group on Numerical Experimentation Report; 32; WMO/TD - No. 1105) [Geneva]: WMO. p. 3.15-3.16.

Watterson, I. G. and Dix, M. R. 2003. Simulated changes due to global warming in daily precipitation means and extremes and their interpretation using the gamma distribution. *J. Geophysical Res*., (in press)..

Watterson, I. G. 2003. Simulated changes due to global warming in the variability of precipitation and their interpretation using a gamma-distributed stochastic model. To be submitted to .

Whetton, P. H., Suppiah. R., McInnees, K. L., Hennessy, K. J. and Jones, R. N. 2002. *Climate Change in Victoria. High resolution regional assessment of climate change impacts.* Department of Natural Resources and Environment, Victoria.